Calorimetric Study of the Glassy State. XIV. Calorimetric Study on Unusual Glass Transition Phenomena in $CFCl_2$-$CFCl_2$

Kōji KISHIMOTO,* Hiroshi SUGA, and Syûzô SEKI

Department of Chemistry, Faculty of Science, Osaka University, Toyonaka, Osaka 560

(Received December 1, 1977)

The heat capacities of the glassy crystalline, plastic crystalline, and liquid phases of $CFCl_2$–$CFCl_2$ were measured by an adiabatic calorimeter over a temperature range from 13 to 310 K, with a sample of 99.93% purity. The triple point was determined to be 297.91 K, the enthalpy and entropy of fusion being 3.666 kJ mol^{-1} and 12.30 J K^{-1} mol^{-1}, respectively. Three kinds of relaxation phenomena were found during the heat capacity measurement centered at around 60, 90, and 130 K, respectively. The first was attributable to the β relaxation. The second was for primary glass transition, where overall rotation or reorientation of the molecules might be frozen. The third was analyzed by ascribing it to the freezing of conversion between the trans and the gauche conformers of the molecule. Activation enthalpy for the internal rotation and energy difference between the two conformers were determined to be 41 kJ mol^{-1} and (790 ± 60) J mol^{-1}, respectively. This experiment provides the first example in which three different freedoms of molecular motion are frozen successively at different temperatures as the crystal is cooled down. An effort to get a possible low-temperature ordered crystalline phase was partially successful by long annealing of the crystal. The extremely sluggish nature of the phase transition into the ordered phase will be related with the slow rate of the internal rotation of the molecule below the transition temperature.

In order to clarify the nature of vitrification process from molecular viewpoint, it is indispensable, at the present stage, to choose as simple a system as possible where degrees of freedom to be taken into account are so restricted in its number that rigorous treatment will be approached. Glassy crystal meets this requirement since it has three-dimensional long-range periodicity which eliminates the complication in considering positional disorder. In hopes of the elucidation of freedoms frozen below a glass transition temperature, T_g, the present material was chosen from the viewpoint of simple molecular structure with internal degrees of definite nature. Kolesov *et al.*[1] already measured the heat capacity of this material and found a type-G transition at around 90 K, according to the phenomenological classification advanced by Guthrie and McCullough.[2] They also reported that this compound has a plastic crystalline phase below its melting point. However, the detailed trend of the heat capacity in the transition region was not delineated in their calorimetric study and they did not mention any relaxational nature of the anomaly. To clarify the nature of the anomaly is the first motivation for the present study. As judged by intuitive plausibility, the transition which they called type-G transition is likely to be a glass transition from the plastic crystal to a glassy crystal. If so, a low-temperature ordered phase must be found by careful thermal treatment. This is another principal object of the study.

Experimental

Material. About 200 g of the compound purchased from E. Merck AG. was first purified by distillation at atmospherric pressure. The middle fraction was subjected to fractional melting in a thermostated bath controllable within $\pm$ 1 mK and then purified by molecular sieve (Linde 3A) to remove low molecular weight compounds as impurities, and finally fractionally distilled *in vacuo*. The calorimeter cell had been attached in advance to the purification system. The purified sample was transferred into the calorimeter cell and then an inlet capillary tubing was pinched off. The analysis of the fractional melting process of the sample, as will be described later, indicated the impurity content of 0.07%.

Heat Capacity Measurement. The heat capacity was measured by the adiabatic calorimeter reported previously.[3] The calorimeter cell was a gold-plated copper can of internal volume 30 cm^3. A sample of 48.121 g (*in vacuo*) was loaded into the cell. No exchange gas was admitted inside the cell. The density of the crystal used in buoyancy correction was calculated from an X-ray diffraction data. A working platium thermometer was calibrated against the International Practical Temperature Scale of 1968 after the completion of the measurement.

X-Ray Diffraction. Preliminary X-ray investigation of the crystal at room temperature was done by the rotating-crystal method. Single crystal was grown from the liquid within a pyrex capillary tubing. X-ray diffraction phtograph was taken at 15 °C by a cylindrical camera of diameter 5.712 cm with Cu K_α radiation

Results and Discussion

X-Ray Diffraction. The observed X-ray diffraction patterns are well indexed as those of the bcc lattice with the cell constant of (0.718 ± 0.004) nm at 15 °C. The rotation photograph has only four reflections, corresponding to (110), (200), (211), and (220) planes, even for prolonged irradiation. This arises from the rapid falling-off in intensity with increasing reflection angle and reflects the fact that the crystal is highly disordered. This behavior is one of the characteristic natures of the plastic crystal.

Determination of Purity. A fractional melting experiment was carried out to determine the melting point and the purity of the sample. In Fig. 1 the reciprocal of the fraction of the sample melted, $1/f$, is plotted against the equilibrium final temperature, T_f, for each energy input. As extremely long time was required for the establishment of thermal equilibrium during the

* Present address: Industrial Research Lab., Kao Soap Co., Ltd., Wakayama.

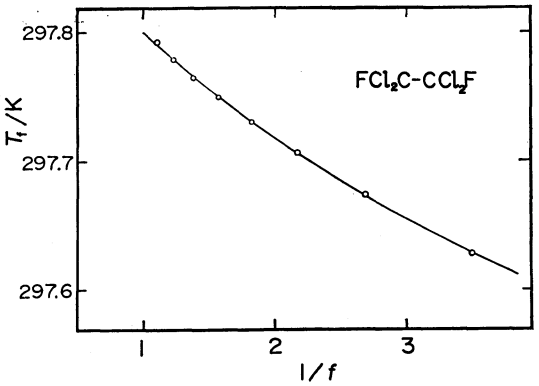

Fig. 1. The equilibrium melting temperature of CCl_2F–CCl_2F plotted against the reciprocal of fraction melted.

TABLE 1. THE EQUILIBRIUM TEMPERATURES DURING FUSION PROCESS OF CCl_2F–CCl_2F

f	$1/f$	T_f/K
0.2856	3.501	297.6273
0.3726	2.684	297.6737
0.4605	2.171	297.7063
0.5491	1.821	297.7305
0.6381	1.567	297.7498
0.7273	1.375	297.7650
0.8167	1.225	297.7789
0.9060	1.104	297.7924

T_{tp}=297.91 K
Purity=99.93%

melting process, the extrapolated value of the temperature to the time being infinite at each energy input was taken as T_f. These values are given in Table 1. Since T_f versus $1/f$ does not yield a straight line, we employed Mastrangelo-Dornte's method[4] in which they derived a solid solution treatment for calorimetric melting point data. By use of this treatment the purity and the triple point of the sample were determined to be 99.93% and 297.91 K, respectively. The enthalpy of fusion was measured twice. These cryoscopic data are given in Table 2. The small entropy of fusion as well as its high crystallographic symmetry indicate that the crystal belongs to the category of plastic crystal originally defined by Timmermans.[5]

TABLE 2. CRYOSCOPIC DATA OF CCl_2F–CCl_2F

T_{tp}/K	ΔH_m/J mol^{-1}	ΔS_m/J K^{-1} mol^{-1}
297.91	3666	12.30

Heat Capacity. The experimental values of the molar heat capacities are listed in Table 3 and presented graphically in Fig. 2. These series of measurements are numbered in chronological order so that their thermal history of the sample may be followed. Also, the approximate temperature increments employed in the measurements may be deduced from the differences in the adjacent average temperatures. Curvature correction was made along the same line as in Ref. 6, whereas the vaporization correction was not made because of

TABLE 3. MOLAR HEAT CAPACITIES OF CCl_2F–CCl_2F

T_{av}/K	C_p/J K^{-1} mol^{-1}	T_{av}/K	C_p/J K^{-1} mol^{-1}
Series 1		229.23	156.05
		232.05	156.68
106.09	132.62	235.02	157.30
108.30	133.05	238.13	158.05
110.64	133.55	241.23	158.95
112.97	133.83	244.31	159.54
115.28	134.36	247.39	160.38
117.55	134.50	250.44	161.14
119.92	135.11	253.35	161.80
122.37	135.62	256.39	162.58
Series 2		Series 6	
127.24	137.13	259.89	163.53
130.09	138.27	263.14	164.33
132.90	139.03	266.37	165.25
135.71	139.05	269.59	166.25
138.50	139.54	272.80	167.13
141.30	139.98	275.99	168.09
144.09	140.49	279.16	169.19
146.84	140.88	282.32	170.20
149.57	141.43	285.46	171.04
152.30	141.83	288.58	172.48
		291.68	173.61
Series 3		294.92	174.74
150.73	141.62	Series 7	
153.56	142.06		
156.41	142.55	279.77	169.28
159.37	143.04	282.97	170.26
162.40	143.52	286.17	171.34
165.42	144.09	289.36	172.67
168.99	144.57	292.54	173.85
Series 4		Series 8	
171.90	145.28	298.96	178.45
174.81	145.52	301.23	178.77
177.69	145.90	304.26	179.20
180.57	146.50	307.29	179.73
183.43	147.05	310.33	180.13
186.27	147.60		
189.10	148.04	Series 9	
191.92	148.68		
194.73	149.06	94.17	130.81
197.51	149.50	96.86	131.29
200.37	150.07	99.53	131.77
203.31	150.67	102.26	132.31
206.24	151.17	105.06	132.65
209.16	152.03		
212.07	152.41	Series 10	
214.96	153.04		
217.84	153.67	115.30	134.24
220.71	154.32	117.63	134.64
223.56	154.85	119.96	135.07
		122.29	135.47
Series 5		124.66	135.94
		127.08	136.39
226.40	155.41	129.53	136.99

Table 3. (Continued)

T_{av}/K	C_p/J K^{-1} mol^{-1}	T_{av}/K	C_p/J K^{-1} mol^{-1}
132.04	138.23	66.40	68.15
134.63	139.29	68.65	69.88
137.34	139.27	70.88	71.63
		73.14	73.49
Series 11		75.42	75.44
		77.78	77.54
158.65	142.81	80.29	80.14
161.32	143.13	82.85	83.41
163.98	145.29	85.31	88.25
166.57	150.60	87.63	99.79
169.18	145.66	89.82	127.66
171.86	145.11	91.96	130.78
174.52	145.55		
		Series 13	
Series 12			
		99.99	129.16
13.93	16.57	103.33	129.82
15.10	18.68	106.63	130.52
16.46	21.18	109.90	131.19
18.20	24.22	113.14	131.93
20.09	27.21	116.35	132.61
21.87	29.84	119.54	133.21
23.60	32.25	121.83	133.61
25.38	34.57	124.99	134.51
27.24	36.83	128.11	135.78
29.00	38.75	131.27	136.94
30.88	40.52	134.50	137.53
32.83	42.37	137.70	137.85
34.69	44.01	140.88	138.51
36.66	45.56	144.05	139.10
38.66	47.23	147.74	139.80
40.59	48.60	150.88	140.53
42.53	50.01	153.99	141.34
44.49	51.40		
46.38	52.69	Series 14	
48.26	53.99		
50.21	55.35	157.36	142.11
52.32	56.79	160.41	143.60
54.48	58.36	163.65	151.37
56.70	59.99	166.68	210.52
59.13	61.84	169.32	213.47
61.65	63.90	172.33	149.40
64.07	66.06	175.51	146.21

lack of the vapor pressure data. As is seen in Fig. 2, the plastic crystal is easily brought into a glassy crystalline state through a glass transition region centered around 90 K. This is really a glass transition phenomenon since the characteristic enthalpy relaxation was observed at this temperature region, as will be shown later. The heat capacities of the glassy crystal plotted in Fig. 2 are for the sample cooled at the rate of 0.2 K min^{-1} from 210 K to temperatures below T_g.

Usually plastic crystal undergoes a transformation on cooling to different phase with ordered molecular orientation in accord with the third law of thermodynamics. The expected ordered phase, however, can not be realized in this crystal by a simple cooling. Therefore,

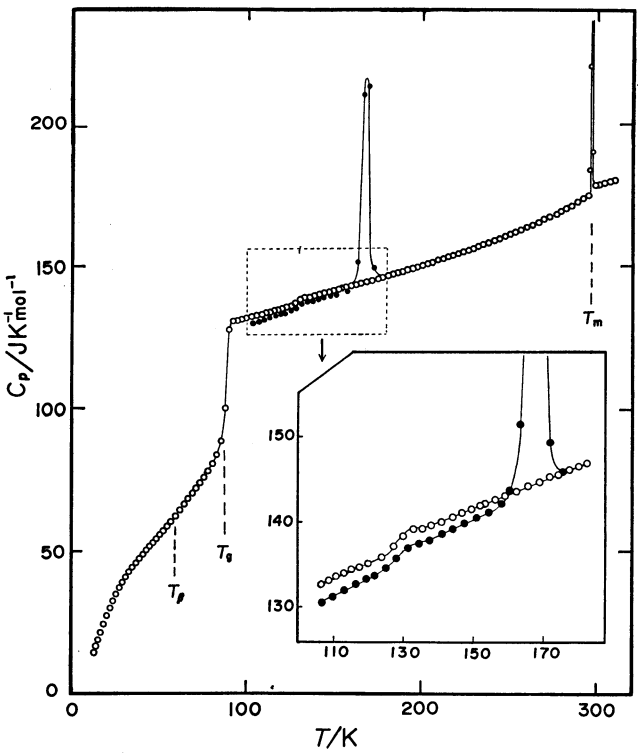

Fig. 2. The heat capacities of CCl_2F–CCl_2F.
○; Rapidly cooled specimen,
●; annealed specimen for 50 days below 120 K.

the sample was first cooled down to 13 K and then annealed in the temperature range between 77 and 160 K for 50 days. This thermal treatment proves to be partially successful for inducing a low-temperature phase. The major feature of the heat capacity for this sample (solid circle in Fig. 2) is a sharp peak at 170 K which is undoubtedly the transition point T_t, separating an ordered and the plastic phases. Extremely long equilibration time was required during the phase transition, and this indicates the first order nature of the transition. The heat capacities below T_t are 0.9% smaller than those for the supercooled plastic crystalline phase, while above T_t both of the values agree within the experimental precision.

The heat capacities of the glassy crystal and its simple extrapolation to higher temperatures serve as an approximation to those for the ordered crystal. Comparing the heat capacity lowering of 0.9% with the heat capacity jump at T_g, it is estimated that 2—3% of the plastic crystalline phase was transformed into the ordered phase by the above thermal treatment. On the other hand, fewer (≈0.16%) ordered phase was obtained by the same procedure except that the sample had not been cooled down to 13 K. Being cooled down to the liquid hydrogen temperature seems to be indispensable for some other kinds of materials to produce their ordered phases as suggested by Finke and Messerly.[7] The fact that the rate of nucleation is accelerated by cooling the crystal to 13 K supports the prevailing idea that some kinds of molecular rearrangement still occur even below T_g. This suggests a potential existence of another relaxation phenomenon below the primary glass transition.

Thermodynamic Functions. Thermodynamic func-

TABLE 4. THERMODYNAMIC FUNCTIONS OF CCl_2F–CCl_2F

T / K	C_p / J K^{-1} mol^{-1}	$S°-S°_0$ / J K^{-1} mol^{-1}	$(H°-H°_0)/T$ / J K^{-1} mol^{-1}	$-(G°-H°_0)/T$ / J K^{-1} mol^{-1}
		Glassy crystalline and Plastic crystalline phases		
10	(8.866)	(3.466)	(2.543)	(0.923)
20	27.11	15.43	10.43	5.00
30	39.69	28.99	18.24	10.75
40	48.19	41.64	24.72	16.91
50	55.19	53.15	30.12	23.03
60	62.53	63.84	34.90	28.94
70	70.96	74.13	39.46	34.67
80	79.83	84.15	43.92	40.23
90	128.13	95.07	49.38	45.69
100	131.79	108.85	57.53	51.32
110	133.42	121.49	64.35	57.14
120	135.05	133.17	70.18	62.99
130	138.26	144.08	75.27	68.81
140	139.80	154.38	79.82	74.56
150	141.45	164.08	83.88	80.21
160	143.09	173.26	87.53	85.74
170	144.77	181.99	90.84	91.15
180	146.47	190.31	93.89	96.43
190	148.19	198.28	96.70	101.58
200	150.05	205.93	99.32	106.61
210	152.03	213.29	101.78	111.51
220	154.09	220.41	104.11	116.30
230	156.23	227.31	106.33	120.98
240	158.50	234.01	108.46	125.55
250	160.96	240.53	110.51	130.02
260	163.61	246.89	112.50	134.39
270	166.40	253.12	114.44	138.67
273.15	167.31	255.05	115.05	140.00
280	169.33	259.22	116.35	142.87
290	172.37	265.22	118.23	146.99
		Liquid phase		
300	178.59	283.43	132.33	151.11
310	180.09	289.32	133.85	155.47

tions at regular temperature intervals were obtained by numerical integration of the smoothed values of the experimental heat capacities. They are all tabulated in Table 4. In the derivation of these apparent thermodynamic functions, the glassy crystalline phase at 0 K was taken as a reference state instead of a crystalline phase which obeys the third law of thermodynamics, because of the failure in preparing pure low-temperature ordered phase. Below 13 K, the values of heat capacity contributing to the thermodynamic functions were calculated on the basis of the effective frequency distribution[8,9] given in the inset in Fig. 3.

Primary and β Relaxation. β relaxation was first observed calorimetrically in the glassy state of isopropylbenzene.[8] An analogous thermal anomaly was observed in the glassy crystalline state of the present material. Figure 4 represents the thermal drifts encountered during the course of heat capacity measurement. These drifts of the calorimeter temperature are the sum of the quasi-adiabatic drifts due to small heat leakage in the calorimetric system and the drifts due to enthalpy relaxations which are responsible for configurational or other changes possibly occurring in the sample. The values shown in this figure are corresponding to the initial drifts taken just after a uniform distribution of the calorimetric temperature which is realized about 5 min after an energy input. Changes in signs of the temperature drifts on heating from exothermic to endothermic ones characteristic of enthalpy relaxation phenomena were observed centering at around 60, 90, and 130 K. The change found around 60 K is attributed to the β relaxation. Associated with this relaxation, the heat capacity increases stepwise by amount of ≈2 J K^{-1} mol^{-1} around 60 K. Figure 3 indicates the excess heat capacity responsible for the β relaxation over those extrapolated from below T_β (see Fig. 2). This extrapolation was carried out by employing the method of effective frequency distribution[8,9] with 22 values for C_p between 14 and 52 K. The inset in this figure is the effective frequency distribution which reproduces best the heat capacity data below 52 K. The nature and the possible origins of β relaxations in glassy liquid and glassy crystal were discussed by Johari[10] based on the dielectric observation. The second found around 90 K in Fig. 4 is attributed to the primary glass transition, where overall rotation or reorientation of molecules might be frozen.

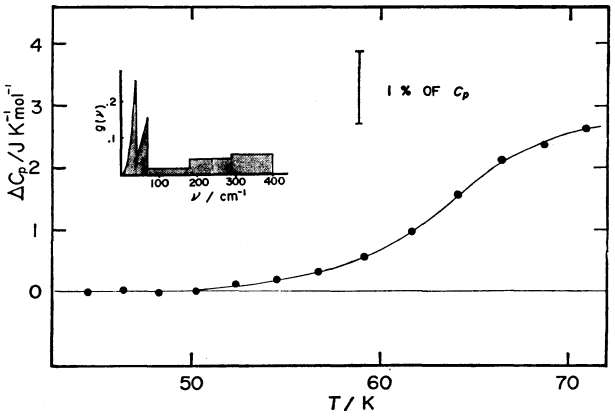

Fig. 3. Excess heat capacities responsible for β relaxation over those extrapolated from T_β.

Anomalous Heat Capacity around 130 K. The heat capacity data above 100 K are reproduced in Fig. 5 on an enlarged scale. The anomalous heat capacities observed around 130 K are accompanied by temperature drifts characteristic of those observed around glass

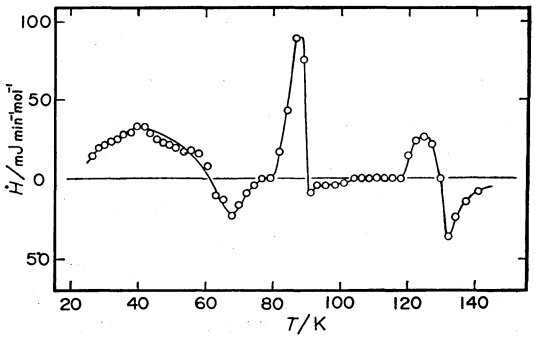

Fig. 4. Spontaneous temperature drifts of calorimeter plotted as a function of temperature.

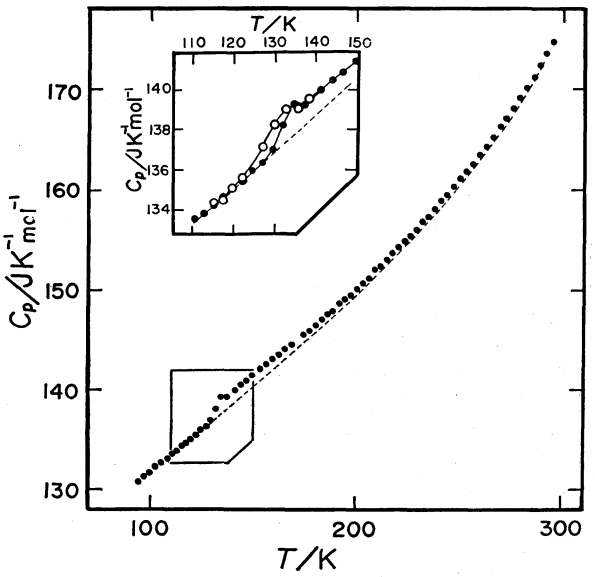

Fig. 5. The heat capacities of CCl_2F–CCl_2F above 100 K on an enlarged scale.
●; Rapidly cooled specimen,
○; annealed specimen at 125 K for about 40 h.

transition region. Taking into account the step-like increase in heat capacity and the nature of temperature drifts, we can conclude that the anomaly arises from relaxational effect of some degrees of freedom. One possible candidate is freezing-in of the conversion between trans and gauche conformers of the molecule. Based on the assumptions that the frequencies of C–C torsional modes are the same for both conformers and that the conversion has little effect on the lattice vibration, the excess heat capacity due to the conversion is approximately described by the Schottky heat capacity.

Newmark and Graves[11] found that the energy of the gauche conformer was 690 J mol^{-1} above the trans conformer in a mixed solvent $CFCl_3$–CF_2Cl_2. Newmark and Sederholm[12] obtained the value 510 J mol^{-1} for the energy difference in $CFCl_3$ solution. Therefore the trans conformer was assumed to be more stable one in the plastic crystalline phase. Then, the molar Schottky heat capacity C_{sch} is given by the following equation:

$$C_{sch} = \frac{\Delta H^2 \exp(\Delta H/RT)}{2RT^2\left[1+\frac{1}{2}\exp(\Delta H/RT)\right]^2}\cdot\theta(T-T_g), \quad (1)$$

where ΔH is the enthalpy difference between the trans and the gauche conformers, R the gas constant, and θ the step function. Below T_g, there exists no contribution to the Schottky heat capacity because of the freezing-in of the conversion. Then, ΔH in this equation can be obtained from C_{sch} at T_g which is corresponding to the heat capacity jump at T_g in Fig. 5. By taking into account of the irreversible enthalpy relaxation effect, the heat capacity jump is assessed to be (1.1±0.2) J K^{-1} mol^{-1} at 130 K, which gives the value (790±60) J mol^{-1} for ΔH. The broken curve in Fig. 5 represents the heat capacities obtained by subtracting C_{sch} from the measured molar heat capacities. This broken curve gives a reasonable extrapolation of the heat capacity below 130 K up to the triple point. Comparison of our value (790±60) J mol^{-1} with the following three values, that is, (i) ΔH=800 J mol^{-1} obtained by Pethrick *et al.*[13] based on the IR and Raman data of Kagarise *et al.*,[14] (ii) ΔH=690 J mol^{-1} obtained by Newmark and Graves and (iii) ΔH=510 J mol^{-1} by Newmark and Sederholm described above, supports the validity of the proposed model for the explanation of the heat capacity anomaly appeared around 130 K.

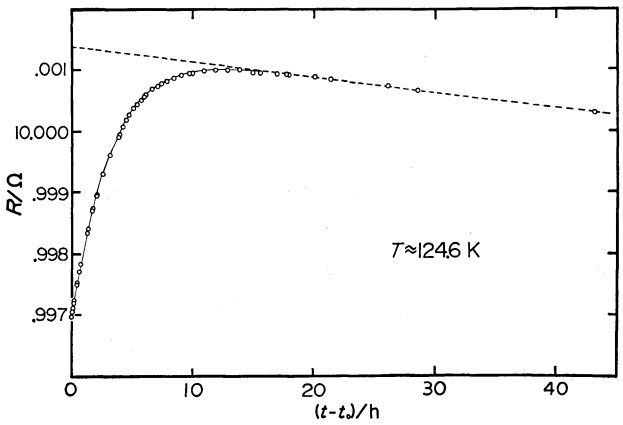

Fig. 6. The temperature drifts due to the enthalpy relaxation phenomenon are plotted as a function of time. The ordinate represents the readings of the platinum resistance thermometer.

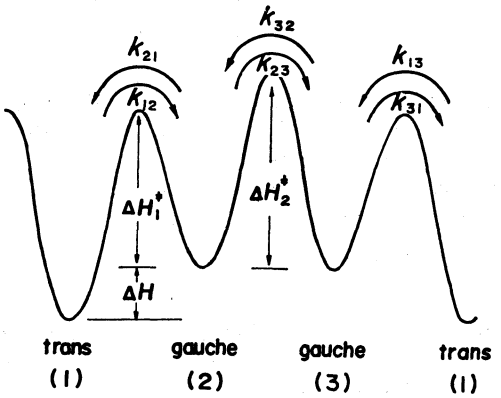

Fig. 7. The enthalpy curve as a function of the coordinate of internal rotation around the C–C bond of CCl_2F–CCl_2F.

The exothermic drifts measured at 124.6 K are plotted in Fig. 6 as a function of time. The broken line indicates the heat leakage caused by the imperfection of adiabatic control. It was assessed to be 28 μW. The difference between the solid and the broken lines is attributed to the enthalpy relaxation inside the specimen, which can be fitted considerably well to an exponential function. The relaxation time at 124.6 K turned out to be 10.4 ks. The process of trans-gauche conversion is very similar to that of unimolecular reactions. In Fig. 7, the states labeled 1, 2, and 3 correspond to trans, gauche, and gauche conformers, respectively. Dynamical equilibrium among them is established above the frozen-in temperature. The transition from state i to state j is assumed to take place with a transition probability k_{ij}.

From the symmetry of the potential function, the following relations can be obtained,

$$k_{32} = k_{23},\ k_{13} = k_{12},\ \text{and}\ k_{31} = k_{21}. \quad (2)$$

Between 1 and 2, and 2 and 3, there exist activated states whose potential barriers have heights of ΔH_1^* and ΔH_2^*, respectively. The rate equation for the occupational probablities of the states may be expressed in a matrix form,

$$\dot{P}(t) = D \cdot P(t), \quad (3)$$

where

$$P(t) = \begin{pmatrix} P_1(t) \\ P_2(t) \\ P_3(t) \end{pmatrix}$$

$$D = \begin{bmatrix} -2k_{12} & k_{21} & k_{21} \\ k_{12} & -(k_{21}+k_{23}) & k_{23} \\ k_{12} & k_{23} & -(k_{21}+k_{23}) \end{bmatrix}. \quad (4)$$

The rate equation has the solution

$$P(t) = (\exp Dt) \cdot P(0) = Te^{At}T^{-1}P(0). \quad (5)$$

T is the matrix that diagonalizes D, and A is the diagonal matrix:

$$A = T^{-1}DT = \begin{bmatrix} 0 & 0 & 0 \\ 0 & -(k_{21}+2k_{12}) & 0 \\ 0 & 0 & -(k_{21}+2k_{23}) \end{bmatrix}. \quad (6)$$

Hence $P(t)$ is readily obtained as

$$P(t) = \begin{bmatrix} P_1^\circ & 2m & 0 \\ P_2^\circ & -m & n \\ P_3^\circ & -m & -n \end{bmatrix} \cdot \begin{pmatrix} 1 \\ \exp(-t/\tau_1) \\ \exp(-t/\tau_2) \end{pmatrix}, \quad (7)$$

where $\tau_1^{-1}=k_{21}+2k_{12}$, $\tau_2^{-1}=k_{21}+2k_{23}$, the coefficients m and n are evaluated from the initial conditions, and P_i° the equilibrium occupational probability of state i.

The internal energy arising from the freedom of internal rotation, H_{int}, is given as follows by taking the trans conformer as the reference state of energy,

$$H_{\text{int}} = \Delta H(P_2+P_3) = \Delta H[2P_2^\circ - 2m\exp(t/\tau_1)]. \quad (8)$$

It is noticeable that the enthalpy relaxation is dominated by a single relaxation time, whereas the dielectric relaxation time for this system is dependent on both τ_1 and τ_2.[15] On the other hand, according to the theory of absolute reaction rate[16] k_{12} can be written in the following form by assuming a transmission coefficient of nearly unity,

$$k_{12} = \frac{kT}{h}\frac{F^*}{F_1}\exp[-(\Delta H_1^* + \Delta H)/RT] \simeq \frac{kT}{h}\left[1-\exp\left(-\frac{h\nu}{kT}\right)\right]\exp[-(\Delta H_1^* + \Delta H)/RT], \quad (9)$$

where F_1 and F^* are the partition functions of the trans conformer for the ground and the activated states, respectively. ν is the C–C torsional frequency, and the other symbols obey the conventional terminology. Similarly, k_{21} and k_{23} are of the form

$$k_{21} \simeq \frac{kT}{h}\left[1-\exp\left(-\frac{h\nu}{kT}\right)\right]\exp\left(-\frac{\Delta H_1^*}{RT}\right),$$

and

$$k_{23} \simeq \frac{kT}{h}\left[1-\exp\left(-\frac{h\nu}{kT}\right)\right]\exp\left(-\frac{\Delta H_2^*}{RT}\right). \quad (10)$$

Assuming $\Delta H \ll \Delta H_1^*$ gives $k_{12}=k_{21}$, and as a result, $\tau_1^{-1} = 3k_{21}$. Equation (8) yields the relation that the enthalpy relaxation time τ is equal to $1/3\,k_{21}$.

ΔH^* can be calculated to be 39.8 kJ mol^{-1} by use of the value 82 cm^{-1} [13] for ν together with the value for τ at 124.6 K. This result agrees well with the value of (38±1) kJ mol^{-1} obtained by Newmark and Graves[11] and of (40±0.4) kJ mol^{-1} obtained by Newmark and Sederholm.[12] The relaxation time at infinite temperature, τ_0, is of the order of 10^{-13} s. The large activation enthalpy in this highly halogenated ethane seems to arise from steric hindrance of the bulky halogen atoms in the eclipsed state. Since all molecules in the low-temperature ordered phase should be in only one and the same conformer, either trans or gauche form, the molecules must rearrange themselves to go to the most stable conformer by exceeding the activated state in the course of the phase transition of the plastic crystalline phase into the ordered phase. Thus one of the reasons for the extremely sluggish nature of the phase transition of the present material seems to be the slow rate of the trans-gauche conversion below T_t (170 K).

The authors express their sincere thanks to Associate Professor Yōzō Chatani for taking the X-ray diffraction photographs

References

1) V. P. Kolesov. V. N. Vorob'ev, and E. A. Sarzhina, *Preprint of Third Intern'l Conf. on Chem. Thermodyn.*, **2**, 33 (1973).
2) G. B. Guthrie and J. P. McCullough, *J. Phys. Chem. Solids*, **18**, 53 (1965).
3) H. Suga and S. Seki, *Bull. Chem. Soc. Jpn.*, **38**, 1000 (1965).
4) S. V. R. Mastrangelo and R. W. Dornte, *J. Am. Chem. Soc.*, **77**, 6200 (1955).
5) J. Timmermans, *J. Phys. Chem. Solids*, **18**, 1 (1961).
6) E. F. Westrum, Jr., G. T. Furukawa, J. P. McCullough, Adiabatic low-temperature calorimetry. In "Experimental Thermodyamics," Vol. 1, ed by J. P. McCullough, D. W. Scott, Butterworths, London (1968).
7) H. L. Finke and J. F. Messerly, *J. Chem. Thermodyn.*, **5**, 247 (1973).
8) K. Kishimoto, H. Suga, and S. Seki, *Bull. Chem. Soc. Jpn.*, **46**, 3020 (1973).
9) M. Sorai and S. Seki, *J. Phys. Soc. Jpn.*, **32**, 382 (1972).
10) G. P. Johari, *Ann. New York Acad. Sci.*, **279**, 117 (1976).
11) R. A. Newmark and E. R. Graves, *J. Phys. Chem.*, **72**, 4299 (1968).
12) R. A. Newmark and C. H. Sederholm, *J. Chem. Phys.*, **43**, 602 (1965).
13) R. A. Pethrick and E. Wyn-Jones, *J. Chem. Soc., Ser. A*, **1971**, 54.
14) R. E. Kagarise and W. Daasch, *J. Chem. Phys.*, **23**, 113 (1955).
15) K. Kishimoto, Doctoral Thesis, Osaka University, 1976. The dipole moment correlation function $\Gamma(t)$ for this system is given by the following equation,

$$\Gamma(t) = \frac{3}{2}P_2^\circ + \frac{3}{4}P_1^\circ\exp(-t/\tau_1) + \frac{1}{4}\exp(-t/\tau_2).$$

16) S. Glasstone, K. S. Laidler, and H. Eyring, "Theory of Rate Process" McGraw-Hill Book Co., Inc., New York (1941).